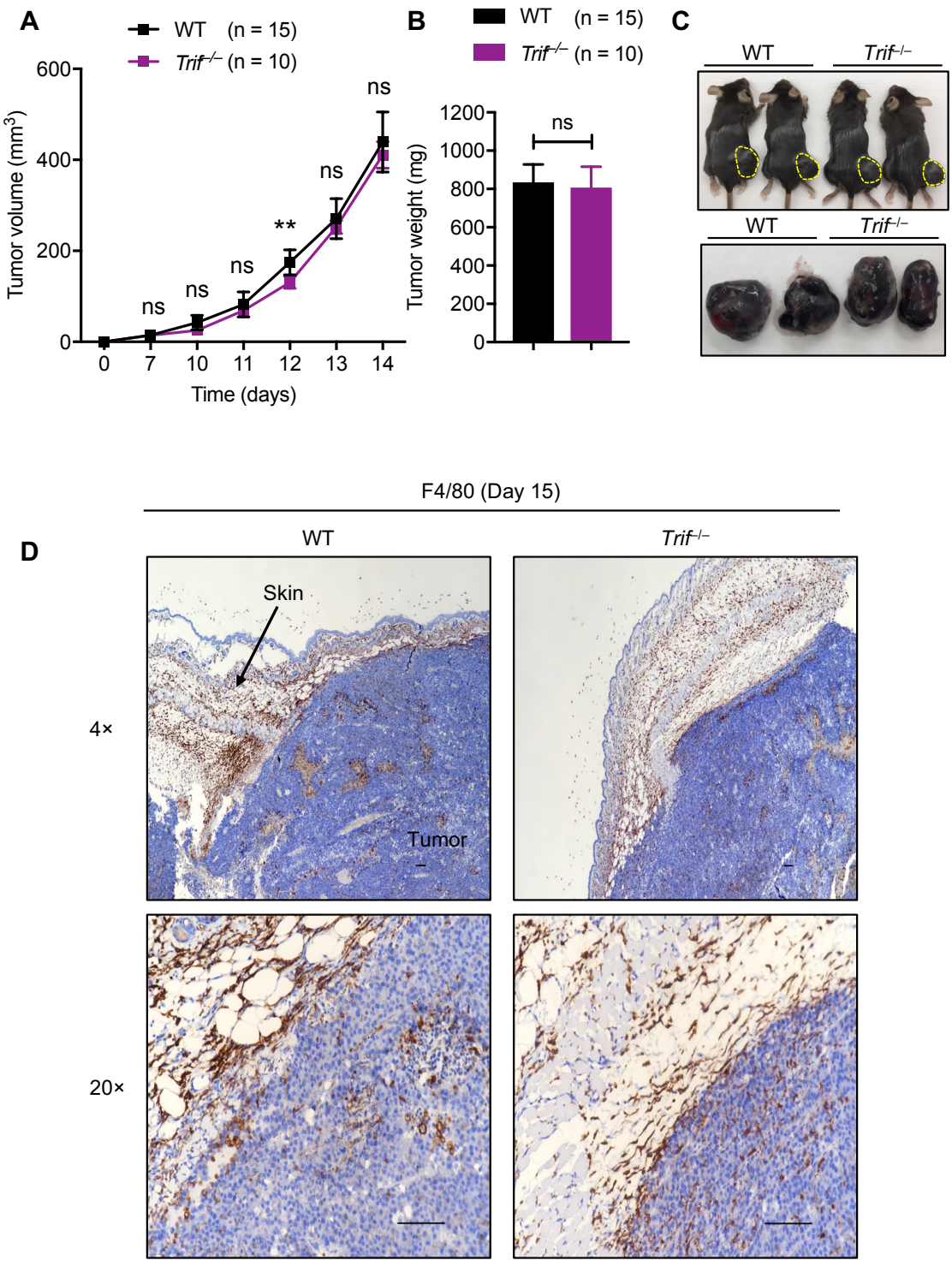

Supplementary Figure S1: Microbiome and Trif are dispensable for melanoma tumor progression.

A–D, B16-F10 melanoma cells were injected into WT and *Trif*$^{-/-}$ mice. **(A)** Mean tumor volume in WT (n = 15) and *Trif*$^{-/-}$ (n = 10) mice. **(B)** Tumor weights of WT (n = 15) and *Trif*$^{-/-}$ (n = 10) mice, 2 weeks after tumor cell injection. **(C)** Representative pictures of tumors from WT and *Trif*$^{-/-}$ mice. **(D)** Immunohistochemistry staining of tumors with F4/80 harvested from WT (n = 5) and *Trif*$^{-/-}$ (n = 5) mice. (Scale bar, 100 μm).

Data are presented as mean ± SD. **(A)** Two-way ANOVA with Sidak's multiple comparison test and **(B)** unpaired *t*-test with Welch's correction were used to determine the significance between the two groups analyzed. ns, not significant $^{**}P < 0.01$.

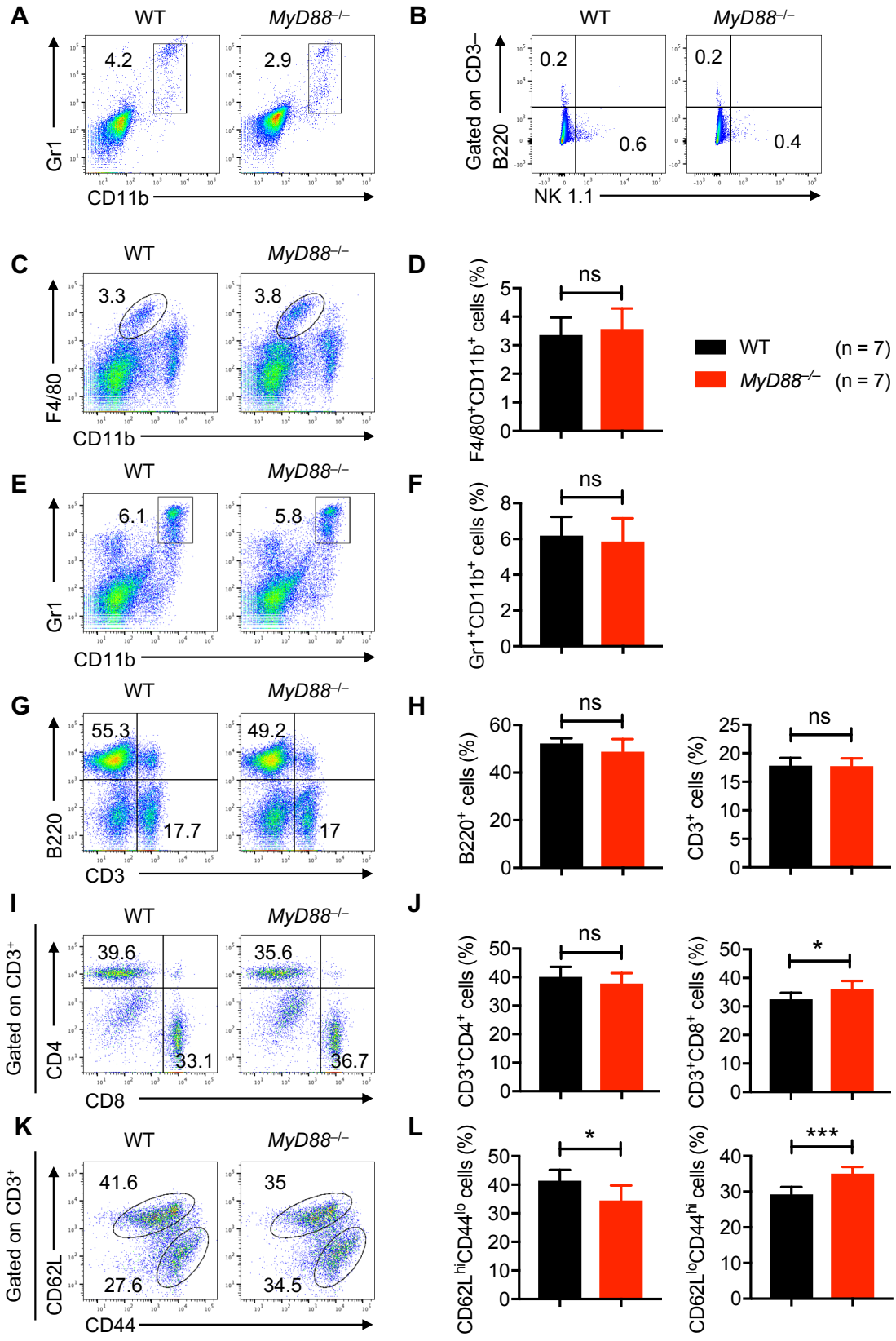

Supplementary Figure S2: Tumor and splenic immune cell populations in *MyD88*$^{-/-}$ mice

bearing melanoma.

A–B, Flow cytometry analysis of immune cell populations in tumors harvested from WT (n = 7) and *MyD88*$^{-/-}$ (n = 7) mice. **(A)** Pseudocolor plots of the Gr1^{+}CD11b^{+} granulocyte population. **(B)** Pseudocolor plots of B220^{+} B-cell and NK1.1^{+} NK-cell populations.

C–L, Flow cytometry analysis of immune cell populations in spleens harvested from WT (n = 7) and *MyD88*$^{-/-}$ (n = 7) mice. **(C)** Pseudocolor plots of F4/80^{+}CD11b^{+} macrophage population. **(D)** Quantification of the F4/80^{+}CD11b^{+} macrophage population. **(E)** Pseudocolor plots of the Gr1^{+}CD11b^{+} granulocyte population. **(F)** Quantification of the Gr1^{+}CD11b^{+} granulocyte population. **(G)** Pseudocolor plots of the B220^{+} B-cell and CD3^{+} T-cell populations. **(H)** Quantification of the B220^{+} B-cell and CD3^{+} T-cell populations. **(I)** Pseudocolor plots of the CD3^{+}CD4^{+} and CD3^{+}CD8^{+} T-cell populations. **(J)** Quantification of the CD3^{+}CD4^{+} and CD3^{+}CD8^{+} T-cell populations. **(K)** Pseudocolor plots of the CD62L^{hi}CD44^{lo} naïve and CD62L^{lo}CD44^{hi} effector T-cell populations. **(L)** Quantification of the CD62L^{hi}CD44^{lo} naïve and CD62L^{lo}CD44^{hi} effector T-cell populations.

Data are presented as mean ± SD. Unpaired *t*-test, with Welch's correction, was used to determine the statistical significance between the two groups analyzed. ns, not significant, **P* < 0.05, ****P* < 0.001.

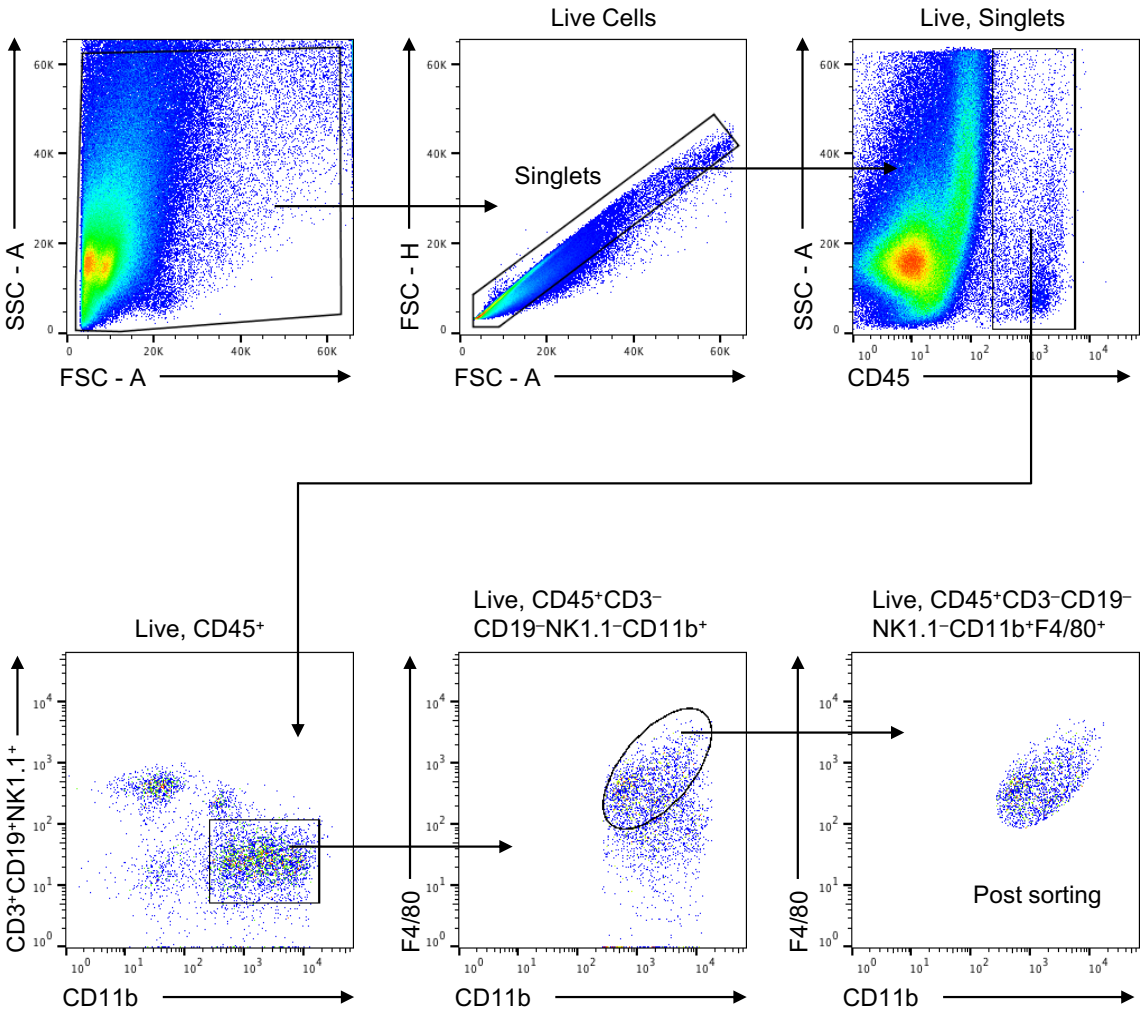

Supplementary Figure S3: FACS gating strategy for sorting the TAM population in tumors.

Debris and doublets were removed, then TAMs were sorted as the $CD45^{+}CD3^{-}CD19^{-}NK1.1^{-}CD11b^{+}F4/80^{+}$ population.

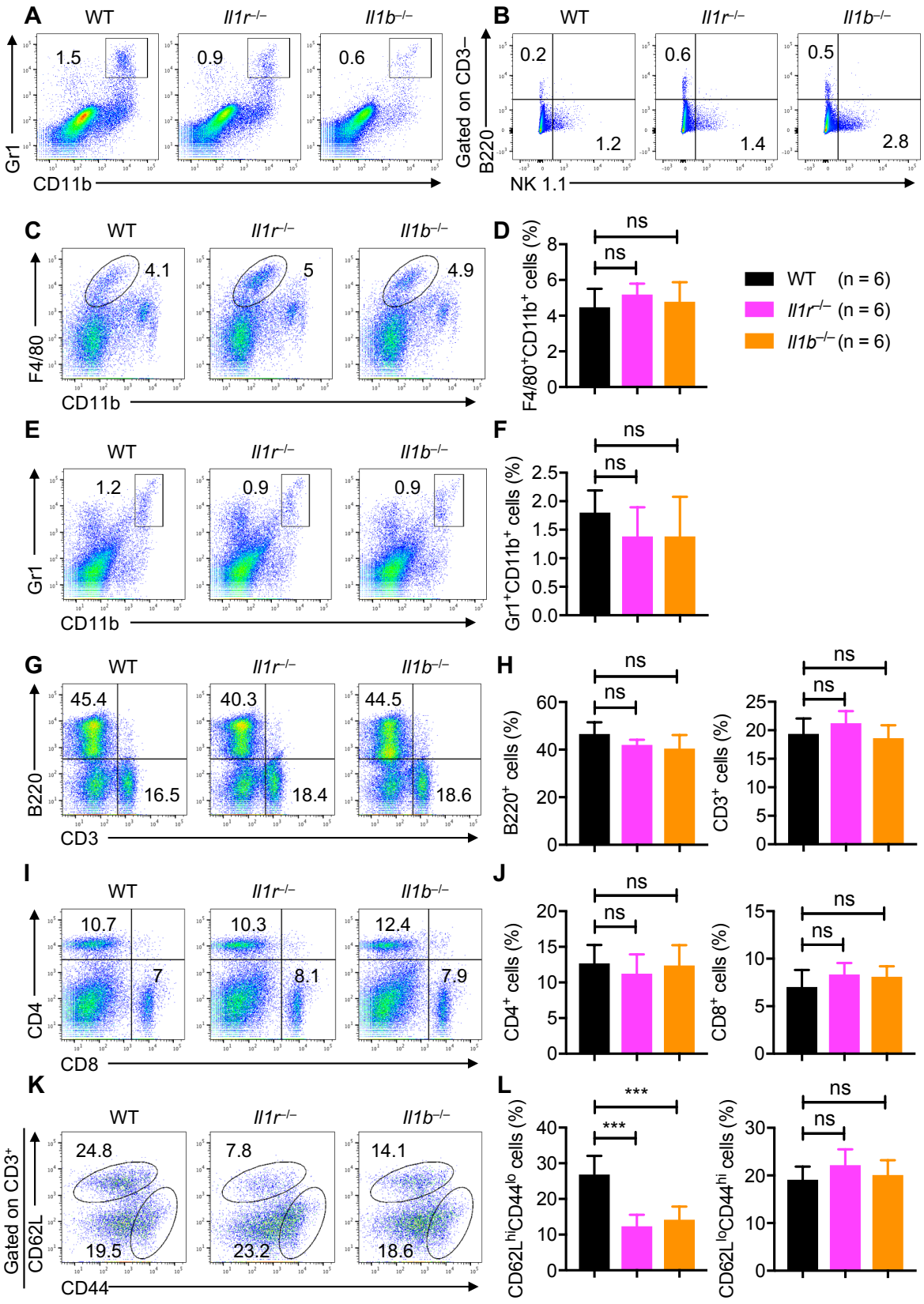

Supplementary Figure S4: Tumor and splenic immune cell populations in IL-1R– or IL-1β–

deficient mice bearing melanoma.

A–B, Flow cytometry analysis of immune cell populations in tumors harvested from WT (n = 6), *Il1r*$^{-/-}$ (n = 6) and *Il1b*$^{-/-}$ (n = 6) mice. **(A)** Pseudocolor plots of the Gr1^{+}CD11b^{+} granulocyte population. **(B)** Pseudocolor plots of B220^{+} B-cell and NK1.1^{+} NK-cell populations.

C–L, Flow cytometry analysis of immune cell populations in spleens harvested from WT (n = 6), *Il1r*$^{-/-}$ (n = 6) and *Il1b*$^{-/-}$ (n = 6) mice. **(C)** Pseudocolor plots of the F4/80^{+}CD11b^{+} macrophage population. **(D)** Quantification of the F4/80^{+}CD11b^{+} macrophage population. **(E)** Pseudocolor plots of the Gr1^{+}CD11b^{+} granulocyte population. **(F)** Quantification of the Gr1^{+}CD11b^{+} granulocyte population. **(G)** Pseudocolor plots of the B220^{+} B-cell and CD3^{+} T-cell populations. **(H)** Quantification of the B220^{+} B-cell and CD3^{+} T-cell populations. **(I)** Pseudocolor plots of the CD4^{+} and CD8^{+} T-cell populations. **(J)** Quantification of the CD4^{+} and CD8^{+} T-cell populations. **(K)** Pseudocolor plots of the CD62L^{hi}CD44^{lo} naïve and CD62L^{lo}CD44^{hi} effector T-cell populations. **(L)** Quantification of the CD62L^{hi}CD44^{lo} naïve and CD62L^{lo}CD44^{hi} effector T-cell populations.

Data are presented as mean ± SD. Unpaired *t*-test, with Welch's correction, was used to determine the statistical significance between the two groups analyzed. ns, not significant, ***P < 0.001.

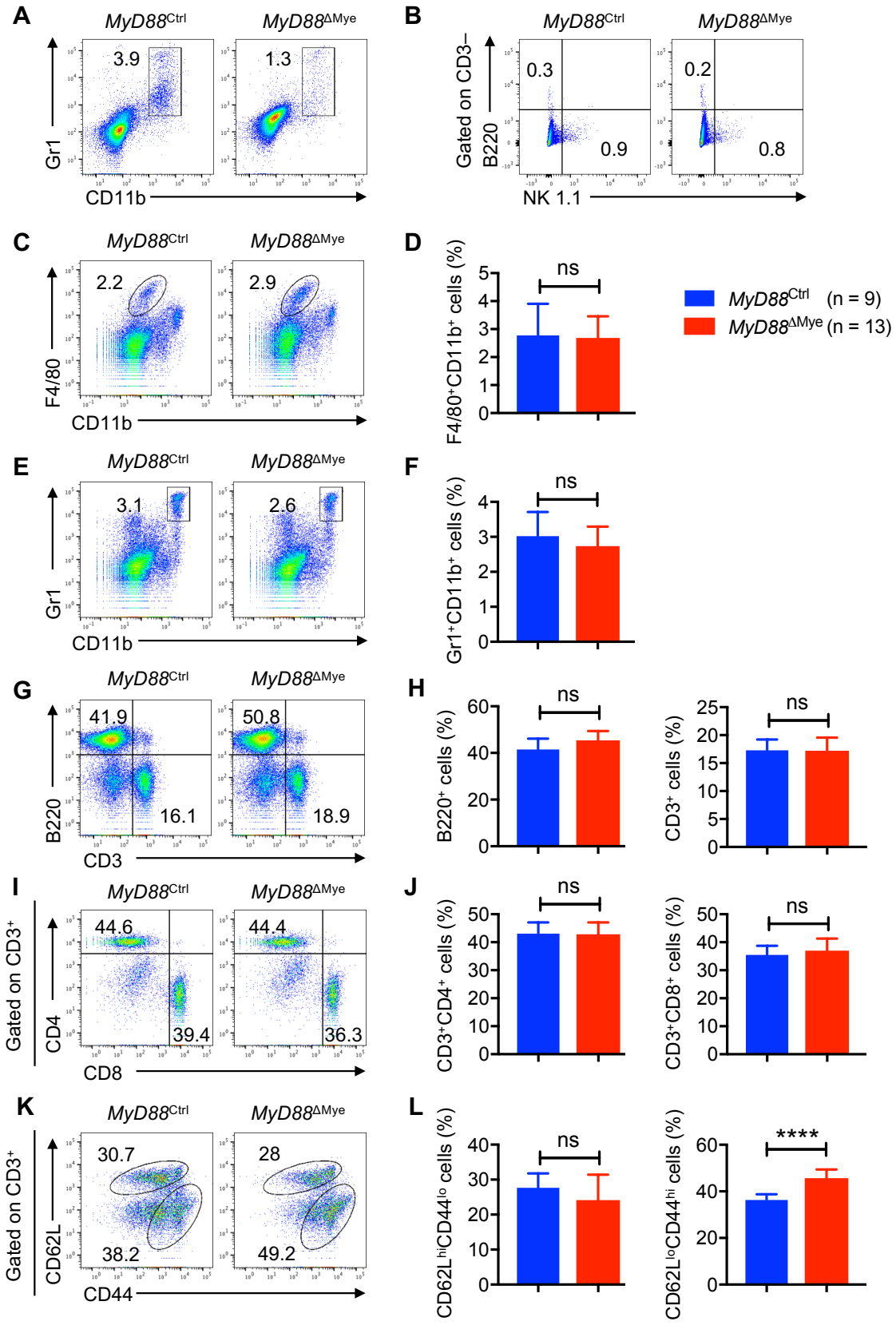

Supplementary Figure S5: Tumor and splenic immune cell populations in *MyD88*$^{\Delta Mye}$ mice

bearing melanoma.

A–B, Flow cytometry analysis of immune cell populations in tumors harvested from *MyD88*^{Ctrl} (n = 9) and *MyD88*$^{\Delta Mye}$ (n = 13) mice. **(A)** Pseudocolor plots of the Gr1^{+}CD11b^{+} granulocyte population. **(B)** Pseudocolor plots of B220^{+} B-cell and NK1.1^{+} NK-cell populations.

C–L, Flow cytometry analysis of immune cell populations in spleens harvested from *MyD88*^{Ctrl} (n = 9) and *MyD88*$^{\Delta Mye}$ (n = 13) mice. **(C)** Pseudocolor plots of the F4/80^{+}CD11b^{+} macrophage population. **(D)** Quantification of the F4/80^{+}CD11b^{+} macrophage population. **(E)** Pseudocolor plots of the Gr1^{+}CD11b^{+} granulocyte population. **(F)** Quantification of the Gr1^{+}CD11b^{+} granulocyte population. **(G)** Pseudocolor plots of the B220^{+} B-cell and CD3^{+} T-cell populations. **(H)** Quantification of the B220^{+} B-cell and CD3^{+} T-cell populations. **(I)** Pseudocolor plots of the CD3^{+}CD4^{+} and CD3^{+}CD8^{+} T-cell populations. **(J)** Quantification of the CD3^{+}CD4^{+} and CD3^{+}CD8^{+} T-cell populations. **(K)** Pseudocolor plots of the CD62L^{hi}CD44^{lo} naïve and CD62L^{lo}CD44^{hi} effector T-cell populations. **(L)** Quantification of the CD62L^{hi}CD44^{lo} naïve and CD62L^{lo}CD44^{hi} effector T-cell populations.

Data are presented as mean ± SD. Unpaired *t*-test, with Welch's correction, was used to determine the statistical significance between the two groups analyzed. ns, not significant, ****$P < 0.0001$.

Supplementary Table S1: Average FPKM values of genes in the study analyzed in various cancers.

	Melanoma n = 102	**Breast Cancer** n = 1075	**Colorectal Cancer** n = 597	**Ovarian Cancer** n = 373	**Lung Cancer** n = 994	**Stomach Cancer** n = 354
MYD88	16.2	18.3	22.5	18.6	17.5	26
TIRAP	2.3	2.6	2.3	1.3	2.1	3.6
TICAM1	10.5	10.6	14.9	10.4	11.4	18.3
TICAM2	0	0	0	0	0	0
MITF	39.2	2.1	0.9	1	1.6	2.3
CEACAM1	15.9	6.7	43.3	2.5	8.2	19.8